

Error Estimation for Δ VLBI Angle and Angle Rate Measurements Over Baselines Between a Ground Station and a Geosynchronous Orbiter

S. C. Wu

Tracking Systems and Applications Section

Baselines between a ground station and a geosynchronous orbiter provide high-resolution Δ VLBI data which is beyond the capability of ground-based interferometry. The effects of possible error sources on such Δ VLBI data for the determination of spacecraft angle and angle rate are investigated. For comparison, the effects on spacecraft-only VLBI are also studied.

I. Introduction and Assumptions

The technology of Δ VLBI over ground baselines for the measurements of deep space probe angle and angle rate has been well developed (Refs. 1-4). Wideband Δ VLBI (or Δ DOR) has been successfully demonstrated using Voyager telemetry subcarrier harmonics near Saturn encounters. It is well known that to resolve the two components of the spacecraft angular position, two nonparallel baselines are needed. These baselines have to be long for a high accuracy, but not too long to have either end of the baseline viewing below a minimum elevation angle ($\sim 10^\circ$). The intercontinental baselines between the three DSN sites at Goldstone, Madrid, and Canberra are nearly optimum in length, although not quite optimum in orthogonality.

To overcome the above limitation, thought has been given to baselines between ground stations and an Earth-orbiting satellite. With proper selection of the satellite geometry, one ground station will suffice. The baseline orthogonality will be furnished by the varying position of the satellite as it orbits around the Earth.

Here we shall investigate the effects of possible error sources on Δ VLBI measurements for the determination of

spacecraft angle and angle rate. The satellite is assumed to be geosynchronous for its unique feature of being in view at all time from a low- or mid-latitude station, provided the inclination of the satellite is not too high. The DSN site at Goldstone (latitude $\sim 35^\circ N$) is selected as the only ground station.

Since most deep space probe trajectories are near the ecliptic plane, which may assume a declination angle between -23 and 23° , an analysis at $\delta = 0^\circ$ will shed enough light on most cases to be encountered in deep space navigation. For this zero- δ case, a low-inclination satellite does not provide a long baseline component in the δ -direction. Therefore, a moderately high inclination angle is desirable. In the following analysis we shall assume a satellite inclination of 45° . For such geometry, the possible baseline projections onto the plane of the sky are shown in Fig. 1 for the two extreme cases and also for a more probable "general" case.

For the "general" case, the satellite orbit plane is inclined from the plane of the sky by an angle of $\sim 63^\circ$. The projections of the two orthogonal baselines are $\sim 40,000$ and $\sim 15,000$ km. These baselines will have error sensitivities of 0.25 and 0.67 nrad/cm, respectively, resulting in an RSS error sensitivity of 0.72 nrad/cm. The RSS error sensitivity will be used in the following estimation of the effects of most

error sources; when the delay (or delay rate) error is a function of the baseline projection length, the effects on angle (or angle rate) will be individually scaled by their component error sensitivities and then RSSed. Such error sources include solar plasma and satellite ephemeris error and spacecraft angular position error in the determination of angle rate.

Table 1 summarizes the assumed geometry and the quantities regarding the system performance and error sources. The rather large separation of 20° between the spacecraft and the quasar is assumed. Such a conservative choice is based on the fact that the number of quasars with correlated flux densities of 0.2 Jansky or higher, over the 40,000-km baseline, is yet to be investigated. We shall study first the effects on angle measurement with wide-band Δ VLBI (bandwidth synthesis) in Section II. Then, in Section III, we shall study the effects on angle rate measurement with narrow-band Δ VLBI. For comparison, we shall also study the cases of spacecraft-only VLBI. Table 2 lists all symbols to be used in the following calculation.

II. Spacecraft Angle Measurement

A. System Noise

The signal-to-noise of the correlated quasar signal can be derived from (Ref. 5)

$$SNR_Q = 2 \times 10^{-4} D_1 D_2 S_c \left(\frac{e_1 e_2 f_{ch} T_{obs}}{T_{s,1} T_{s,2}} \right)^{1/2}$$

$$= 6.8$$

The spacecraft signal is to be correlated individually at each end of the baseline with local models. The corresponding SNR are (Ref. 3)

$$SNR_S = 2 \left(\frac{P_t T_{obs}}{\pi k T} \right)^{1/2}$$

$$= 74.4 \text{ at satellite}$$

and

$$SNR_G = SNR_S \left(\frac{D_2}{D_1} \right) \left(\frac{\epsilon_2 T_1}{\epsilon_1 T_2} \right)^{1/2}$$

$$= 211.9 \text{ at Goldstone}$$

For S/C-only VLBI, the delay error is given by

$$\epsilon_\tau = \frac{\sqrt{2} c}{2\pi f_{span}} \left[\left(\frac{1}{SNR_S} \right)^2 + \left(\frac{1}{SNR_G} \right)^2 \right]^{1/2}$$

$$= 0.96 \text{ cm}$$

and the corresponding angle error is

$$\epsilon_\theta = 0.72 \epsilon_\tau = 0.69 \text{ nrad} \quad (1)$$

For Δ VLBI, the error is dominated by SNR_Q of the quasar signal. Hence the differenced delay error is

$$\epsilon_{\Delta\tau} = \frac{\sqrt{2} c}{2\pi f_{span}} \left(\frac{1}{SNR_Q} \right)$$

$$= 9.93 \text{ cm}$$

The corresponding angular separation error is

$$\epsilon_{\Delta\theta} = 0.72 \epsilon_{\Delta\tau} = 7.15 \text{ nrad} \quad (2)$$

B. Clock Offset

For S/C-only VLBI, the delay error is

$$\epsilon_\tau = c T_{off}$$

$$= 150 \text{ cm}$$

with a corresponding angle error of

$$\epsilon_\theta = 108 \text{ nrad} \quad (3)$$

The differenced delay measured by Δ VLBI is insensitive to clock offset.

C. Frequency Offset

Frequency offset between the two ends of a baseline has an effect on VLBI delay measurement of

$$\epsilon_\tau = \frac{1}{2} \frac{f_{off}}{f_{RF}} c T_{obs}$$

$$= 10.71 \text{ cm}$$

The corresponding angle error is

$$\epsilon_{\theta} = 7.71 \text{ nrad} \quad (4)$$

For Δ VLBI, the effect on the differenced delay is

$$\begin{aligned} \epsilon_{\Delta\tau} &= \frac{f_{off}}{f_{RF}} c T_{S/C-Q} \\ &= 25.71 \text{ cm} \end{aligned}$$

which gives

$$\epsilon_{\Delta\theta} = 18.51 \text{ nrad} \quad (5)$$

D. Clock Instability

For S/C-only VLBI, the delay error is

$$\begin{aligned} \epsilon_{\tau} &= \frac{\sqrt{2} c T_{obs}}{2} \left(\frac{\Delta f}{f} \right) \\ &= 1.28 \text{ cm} \end{aligned}$$

and the angle error is

$$\epsilon_{\theta} = 0.92 \text{ nrad} \quad (6)$$

For Δ VLBI, the differenced delay error is

$$\begin{aligned} \epsilon_{\Delta\tau} &= \sqrt{2} c T_{S/C-Q} \left(\frac{\Delta f}{f} \right) \\ &= 3.07 \text{ cm} \end{aligned}$$

and the angular separation error is

$$\epsilon_{\Delta\theta} = 2.21 \text{ nrad} \quad (7)$$

E. Troposphere

Troposphere (and ionosphere) affects only the ground observations; it has no effect on the observations made from the satellite. For S/C-only VLBI, the delay error is

$$\epsilon_{\tau} = \frac{\rho_z^t}{\sin \gamma_{S/C}} = 14.20 \text{ cm}$$

and the corresponding angle error is

$$\epsilon_{\theta} = 10.22 \text{ nrad} \quad (8)$$

For Δ VLBI, the differenced delay error due to a systematic calibration error is

$$\begin{aligned} \epsilon_{\Delta\tau} &= \rho_z^t \left| \frac{1}{\sin \gamma_{S/C}} - \frac{1}{\sin \gamma_Q} \right| \\ &= 4.86 \text{ cm} \end{aligned}$$

and that due to a horizontal inhomogeneity is

$$\begin{aligned} \epsilon_{\Delta\tau} &= \frac{\rho_{inh}^t}{\sin \gamma_{S/C}} \\ &= 4.73 \text{ cm} \end{aligned}$$

The corresponding angular separation error is

$$\epsilon_{\Delta\theta} = 4.89 \text{ nrad} \quad (9)$$

F. Ionosphere

For S/C-only VLBI, the delay error due to a calibration error in ionospheric peak delay is

$$\begin{aligned} \epsilon_{\tau} &= \rho_{peak}^i f(X_{S/C}) g(\gamma_{S/C}) \\ &= 2.35 \text{ cm} \end{aligned}$$

where the solar-zenith angle factor $f(X)$ and the elevation angle factor $g(\gamma)$ are given in Fig. 2 (Ref. 6).

The delay error due to a bias ionospheric error is

$$\begin{aligned} \epsilon_{\tau} &= \rho_{bias}^i g(\gamma) \\ &= 5.91 \text{ cm} \end{aligned}$$

The angle error is calculated to be

$$\epsilon_{\theta} = 4.58 \text{ nrad} \quad (10)$$

For Δ VLBI the differenced delay error due to an ionospheric peak error is

$$\epsilon_{\Delta\tau} = \rho_{peak}^i [f(X_{S/C}) g(\gamma_{S/C}) - f(X_Q) g(\gamma_Q)]$$

$$= 0.66 \text{ cm}$$

that due to a bias error is

$$\epsilon_{\Delta\tau} = \rho_{bias}^i [g(\gamma_{S/C}) - g(\gamma_Q)]$$

$$= 1.53 \text{ cm}$$

and that due to a spatial fluctuation is

$$\epsilon_{\Delta\tau} = \rho_{spa}^i f(X_{S/C}) g(\gamma_{S/C})$$

$$= 4.73 \text{ cm}$$

The angular separation error from these three error types is

$$\epsilon_{\Delta\theta} = 3.61 \text{ nrad} \quad (11)$$

G. Solar Plasma

The cancellation of solar plasma effect between two ray paths degrades as the ray path separation increases. Hence the effect on VLBI delay measurement is larger for longer baseline projection: For the longer baseline (40,000 km), the delay error is (Ref. 7)

$$\epsilon_{\tau} = 0.052 \left(\frac{B}{V_{SW}} \right)^{0.75} [10 \sin(SEP)]^{-1.3}$$

$$= 0.80 \text{ cm}$$

which corresponds to an angle error of

$$\epsilon_{\theta} = 0.25 \quad \epsilon_{\tau} = 0.20 \text{ nrad}$$

For the shorter baseline (15,000 km)

$$\epsilon_{\tau} = 0.38 \text{ cm}$$

and

$$\epsilon_{\theta} = 0.67 \quad \epsilon_{\tau} = 0.26 \text{ nrad}$$

The 2-D angle error is

$$\epsilon_{\theta} = 0.33 \text{ nrad} \quad (12)$$

For Δ VLBI with a source separation of 20° , the separation at solar plasma distance (~ 1 AU) between ray paths observing S/C and quasar from the same site is much greater than that between the two sites observing the same source. Hence only common-source cancellation is effective. The Δ VLBI angle separation error is $\sqrt{2}$ as large as in the case of S/C-only VLBI:

$$\epsilon_{\Delta\theta} = \sqrt{2} \epsilon_{\theta} = 0.47 \text{ nrad} \quad (13)$$

H. Station Location Error

For S/C-only VLBI measurement,

$$\epsilon_{\tau} = \epsilon_{STN} = 50 \text{ cm}$$

and

$$\epsilon_{\theta} = 36.00 \text{ nrad} \quad (14)$$

For Δ VLBI measurement, it can be shown that

$$\epsilon_{\Delta\tau} = [(\Delta\alpha \cos \delta)^2 + (\Delta\delta)^2]^{1/2} \epsilon_{STN}$$

$$= 17.45 \text{ cm}$$

and

$$\epsilon_{\Delta\theta} = 12.57 \text{ nrad} \quad (15)$$

I. Satellite Position Error

For S/C-only VLBI measurement, the delay error accompanying the longer baseline is

$$\epsilon_{\tau} = [(\epsilon_L \sin \Omega)^2 + (\epsilon_C \cos \Omega)^2]^{1/2}$$

$$= 271.13 \text{ cm}$$

corresponding to an angle error of

$$\epsilon_{\theta} = 0.25 \quad \epsilon_{\tau} = 67.78 \text{ nrad}$$

The delay error accompanying the shorter baseline is

$$\epsilon_{\tau} = [(\epsilon_H \sin \Omega)^2 + (\epsilon_C \cos \Omega)^2]^{1/2}$$

$$= 100 \text{ cm}$$

corresponding to an angle error of

$$\epsilon_{\theta} = 0.67 \epsilon_{\tau} = 67 \text{ nrad}$$

The 2-D angle error is

$$\epsilon_{\theta} = 95.31 \text{ nrad} \quad (16)$$

For Δ VLBI measurement, the angular separation error is reduced by the separation angle:

$$\epsilon_{\Delta\theta} = \Delta\theta \epsilon_{\theta} = 33.27 \text{ nrad} \quad (17)$$

J. Phase Instability

For S/C-only VLBI measurement, the effect is

$$\begin{aligned} \epsilon_{\tau} &= \frac{2c}{2\pi f_{span}} \epsilon_{\phi} \\ &= 3.33 \text{ cm} \end{aligned}$$

and

$$\epsilon_{\theta} = 2.40 \text{ nrad} \quad (18)$$

For Δ VLBI the effect is estimated to have the same magnitude as that on VLBI measurement:

$$\epsilon_{\Delta\theta} = \epsilon_{\theta} = 2.40 \text{ nrad} \quad (19)$$

K. Quasar Position Error

This error affects only Δ VLBI measurements:

$$\epsilon_{\Delta\theta} = \epsilon_{\theta,Q} = 5 \text{ nrad} \quad (20)$$

III. Spacecraft Angle Rate Measurement

A. System Noise

The effect on S/C-only VLBI measurement is very small and can be ignored. The effect on Δ VLBI is dominated by the correlated quasar signal-to-noise ratio,

$$\begin{aligned} \epsilon_{\Delta\dot{\tau}} &= \frac{4c}{2\pi f_{RF} T_{obs}} \left(\frac{1}{SNR_Q} \right) \\ &= 0.56 \times 10^{-3} \text{ cm/sec} \end{aligned}$$

and the corresponding angle rate error is

$$\epsilon_{\Delta\dot{\theta}} = 0.40 \text{ prad/sec} \quad (21)$$

B. Clock Offset

Clock offset between the two ends of a baseline has no effect on either VLBI or Δ VLBI measurements.

C. Frequency Offset

For S/C-only VLBI measurement, the delay rate error is

$$\epsilon_{\dot{\tau}} = \frac{f_{off}}{f_{RF}} c = 35.71 \times 10^{-3} \text{ cm/sec}$$

which corresponds to an angle rate error of

$$\epsilon_{\dot{\theta}} = 25.71 \text{ prad/sec} \quad (22)$$

Δ VLBI measurement is insensitive to frequency offset.

D. Clock Instability

For S/C-only VLBI measurement, the delay rate error is

$$\begin{aligned} \epsilon_{\dot{\tau}} &= \sqrt{2} c \left(\frac{\Delta f}{f} \right) \\ &= 4.26 \times 10^{-3} \text{ cm/sec} \end{aligned}$$

and the corresponding angle rate error is

$$\epsilon_{\dot{\theta}} = 3.07 \text{ prad/sec} \quad (23)$$

For Δ VLBI measurement, the differenced delay rate error can be shown to be

$$\begin{aligned} \epsilon_{\Delta\dot{\tau}} &= \sqrt{2} c \left(\frac{\Delta f}{f} \right) \left(\frac{T_{S/C-Q}}{T_{obs}} \right)^{1/2} \\ &= 4.67 \times 10^{-3} \text{ cm/sec} \end{aligned}$$

corresponding to an angle rate error of

$$\epsilon_{\Delta\dot{\theta}} = 3.36 \text{ prad/sec} \quad (24)$$

E. Troposphere

For S/C-only VLBI, the delay rate error is

$$\epsilon_{\dot{\tau}} = \left| \frac{\partial}{\partial t} \left(\frac{\rho_z^t}{\sin \gamma_{S/C}} \right) \right| = \rho_z^t \left| \frac{\cos \gamma_{S/C}}{\sin^2 \gamma_{S/C}} \dot{\gamma}_{S/C} \right|$$

Let

$$\dot{\gamma}_{S/C} = 0.7 \omega_e$$

then

$$\epsilon_{\dot{\tau}} = 1.56 \times 10^{-3} \text{ cm/sec}$$

corresponding to an angle rate error of

$$\epsilon_{\dot{\theta}} = 1.12 \text{ prad/sec} \quad (25)$$

For Δ VLBI, let $\dot{\gamma}_Q = 0.6 \omega_e$. The differenced delay rate error due to a systematic error is

$$\begin{aligned} \epsilon_{\Delta\dot{\tau}} &= \rho_z^t \left| \frac{\cos \gamma_{S/C}}{\sin^2 \gamma_{S/C}} \dot{\gamma}_{S/C} - \frac{\cos \gamma_Q}{\sin^2 \gamma_Q} \dot{\gamma}_Q \right| \\ &= 1.07 \times 10^{-3} \text{ cm/sec} \end{aligned}$$

and that due to a horizontal inhomogeneity is

$$\begin{aligned} \epsilon_{\Delta\dot{\tau}} &= \rho_{inh}^t \left| \frac{\cos \gamma_{S/C}}{\sin^2 \gamma_{S/C}} \dot{\gamma}_{S/C} \right| \\ &= 0.52 \times 10^{-3} \text{ cm/sec} \end{aligned}$$

The corresponding angular rate error is

$$\epsilon_{\Delta\dot{\theta}} = 0.86 \text{ prad/sec} \quad (26)$$

F. Ionosphere

On both VLBI and Δ VLBI angle rate measurements, only the temporal fluctuation component of the ionosphere has a significant effect. For S/C-only VLBI,

$$\begin{aligned} \epsilon_{\dot{\tau}} &= \frac{\rho_{temp}^i}{T_{obs}} f(X_{S/C}) g(\gamma_{S/C}) \\ &= 2.63 \times 10^{-3} \text{ cm/sec} \end{aligned}$$

and

$$\epsilon_{\dot{\theta}} = 1.89 \text{ prad/sec} \quad (27)$$

For Δ VLBI measurement,

$$\begin{aligned} \epsilon_{\Delta\dot{\tau}} &= \frac{\rho_{temp}^i}{T_{obs}} [f^2(X_{S/C}) g^2(\gamma_{S/C}) + f^2(X_Q) g^2(\gamma_Q)]^{1/2} \\ &= 3.24 \times 10^{-3} \text{ cm/sec} \end{aligned}$$

and

$$\epsilon_{\Delta\dot{\theta}} = 2.33 \text{ prad/sec} \quad (28)$$

G. Solar Plasma

For S/C-only VLBI, the delay rate measurement over the longer baseline has an error of

$$\begin{aligned} \epsilon_{\dot{\tau}} &= \frac{0.052 \sqrt{2}}{T_{obs}} \left(\frac{B}{V_{SW}} \right)^{0.75} [10 \sin(SEP)]^{-1.3} \\ &= 1.89 \times 10^{-3} \text{ cm/sec} \end{aligned}$$

which is corresponding to an angle rate error of

$$\epsilon_{\dot{\theta}} = 0.47 \text{ prad/sec}$$

Over the shorter baseline, the errors are

$$\epsilon_{\dot{\tau}} = 0.91 \times 10^{-3} \text{ cm/sec}$$

and

$$\epsilon_{\dot{\theta}} = 0.61 \text{ prad/sec}$$

The 2-D angle rate error is

$$\epsilon_{\dot{\theta}} = 0.77 \text{ prad/sec} \quad (29)$$

For Δ VLBI measurement, the error is $\sqrt{2}$ times larger; i.e.,

$$\epsilon_{\Delta\dot{\theta}} = 1.09 \text{ prad/sec} \quad (30)$$

H. Station Location Error

For S/C-only VLBI measurement, the delay rate error is

$$\begin{aligned}\epsilon_{\dot{\tau}} &= \omega_e \epsilon_{STN} \cos \delta \\ &= 3.65 \times 10^{-3} \text{ cm/sec}\end{aligned}$$

and the corresponding angle rate error is

$$\epsilon_{\dot{\theta}} = 2.63 \text{ prad/sec} \quad (31)$$

For VLBI measurement, the differenced delay rate error is

$$\begin{aligned}\epsilon_{\Delta \dot{\tau}} &= \omega_e \epsilon_{STN} [(\Delta \alpha \cos \delta)^2 + (\Delta \delta \sin \delta)^2]^{1/2} \\ &= 1.27 \times 10^{-3} \text{ cm/sec}\end{aligned}$$

and the corresponding angle rate error is

$$\epsilon_{\Delta \dot{\theta}} = 0.92 \text{ prad/sec} \quad (32)$$

I. Satellite Velocity Error

For S/C-only VLBI measurement, the effect on the delay rate measurement over the longer baseline is

$$\begin{aligned}\epsilon_{\dot{\tau}} &= [(\epsilon_{\dot{L}} \sin \Omega)^2 + (\epsilon_{\dot{C}} \cos \Omega)^2]^{1/2} \\ &= 27.11 \times 10^{-3} \text{ cm/sec}\end{aligned}$$

corresponding to an angle rate error of

$$\epsilon_{\dot{\theta}} = 6.78 \text{ prad/sec.}$$

The delay rate error over the shorter baseline is

$$\begin{aligned}\epsilon_{\dot{\tau}} &= [(\epsilon_{\dot{H}} \sin \Omega)^2 + (\epsilon_{\dot{C}} \cos \Omega)^2]^{1/2} \\ &= 10 \times 10^{-3} \text{ cm/sec}\end{aligned}$$

corresponding to an angle rate error of

$$\epsilon_{\dot{\theta}} = 6.70 \text{ prad/sec}$$

The 2-D angle rate error is

$$\epsilon_{\dot{\theta}} = 9.53 \text{ prad/sec} \quad (33)$$

For Δ VLBI measurement, the angle rate error is reduced by the S/C-quasar angular separation:

$$\epsilon_{\Delta \dot{\theta}} = \Delta \theta \epsilon_{\dot{\theta}} = 3.33 \text{ prad/sec} \quad (34)$$

J. Phase Instability

For S/C-only VLBI measurement, the delay rate error is

$$\begin{aligned}\epsilon_{\dot{\tau}} &= \frac{2c}{2\pi f_{RF} T_{obs}} \epsilon_{\phi} \\ &= 0.06 \times 10^{-3} \text{ cm/sec}\end{aligned}$$

which is negligibly small. The error on Δ VLBI measurement is estimated to be of the same magnitude and is also negligible.

K. S/C Angular Position Error

It can be shown that the sensitivity of (differenced) delay rate to such error is equal to the rate of change of the baseline projection in the direction of the angular position (separation) error. That is,

$$\frac{\partial \dot{\tau}}{\partial \theta} = \hat{\theta} \cdot \dot{\mathbf{B}}, \quad \frac{\partial (\Delta \dot{\tau})}{\partial (\Delta \theta)} = \Delta \hat{\theta} \cdot \dot{\mathbf{B}}$$

For S/C-only VLBI, the delay rate error over the longer baseline is

$$\begin{aligned}\epsilon_{\dot{\tau}} &= \omega_e a \cos \Omega \epsilon_{\theta} \\ &= 21.03 \times 10^{-3} \text{ cm/sec}\end{aligned}$$

corresponding to an angle rate error of

$$\epsilon_{\dot{\theta}} = 5.26 \text{ prad/sec}$$

Over the shorter baseline the errors are

$$\begin{aligned}\epsilon_{\dot{\tau}} &= \omega_e a \epsilon_{\theta} \\ &= 46.32 \text{ cm/sec}\end{aligned}$$

and

$$\epsilon_{\dot{\theta}} = 31.03 \text{ prad/sec}$$

The 2-D angle rate error is

$$\epsilon_{\dot{\theta}} = 31.48 \text{ prad/sec} \quad (35)$$

For Δ VLBI measurement, the same calculation applies

except that ϵ_θ is replaced by $\epsilon_{\Delta\theta}$, which is assumed to be a factor of (40/150) smaller. Hence,

$$\epsilon_{\Delta\dot{\theta}} = \left(\frac{40}{150}\right) \epsilon_{\dot{\theta}} = 8.39 \text{ prad/sec} \quad (36)$$

Note that the errors are dominated by a component resulting from S/C angular position error in the direction parallel to the longer baseline.

IV. Summary

Figures 3 and 4 summarize, respectively, the angle and angle rate errors for both S/C-only VLBI and S/C-quasar Δ VLBI data types. The VLBI angle measurement error is

dominated by clock offset and satellite position error, which are unlikely to be greatly reduced. For Δ VLBI angle measurement the major error sources are in satellite position and station location, both of which are scaled by the S/C-quasar angular separation. Hence the RSS error will also be scaled by such separation.

The determination of spacecraft angle rate is extremely sensitive to spacecraft angular position error. In the application to a planetary orbiter, where such data type will most probably be needed, the dynamics of the spacecraft trajectory allows the determination of the angular position. Therefore the effects of angular position error are removed. In the case of a cruising interplanetary spacecraft, the angle rate can be better determined from successive Δ VLBI angle measurements.

References

1. Melbourne, W. G., and Curkendall, D. W., "Radio Metric Direction Finding: A New Approach to Deep Space Navigation," paper presented at AAS/AIAA Astrodynamics Specialist Conference, Jackson Hole, Wyoming, Sep. 1977.
2. Brown, D. S., Hildebrand, C. E., and Skjerve, L. J., "Wideband Δ VLBI For Deep Space Navigation," paper presented at IEEE Position Location and Navigation Symposium, Atlantic City, N.J., Dec. 1980.
3. Brunn, D. L., Preston, R. A., Wu, S. C., Siegel, H. L., Brown, D. S., Christensen, C. S., and Hilt, D. E., " Δ VLBI Spacecraft Tracking System Demonstration: Part I. Design and Planning," *DSN Progress Report 42-45*, pp. 111-132. Jet Propulsion Laboratory, Pasadena, Calif., June 15, 1978.
4. Christensen, C. S., Moultrie, B., Callahan, P. S., Donovan, F. F., and Wu, S. C., " Δ VLBI Spacecraft Tracking System Demonstration: Part II. Data Acquisition and Processing," *TDA Progress Report 42-60*, pp. 60-67, Jet Propulsion Laboratory, Pasadena, Calif., Dec. 15, 1980.
5. Thomas, J. B., *An Analysis of Long Baseline Radio Interferometry, Part II*, Technical Report 32-1526, Vol. VIII, pp. 29-38, Jet Propulsion Laboratory, Pasadena, Calif. Apr. 1972.
6. Wu, S. C., "Atmospheric Media Effects on ARIES Baseline Determination," *TDA Progress Report 42-61*, pp. 1-6, Jet Propulsion Laboratory, Pasadena, Calif., Feb. 15, 1981.
7. Callahan, P. S., "An Analysis of Viking S-X Doppler Measurements of Solar Wind Columnar Content Fluctuation," *DSN Progress Report 42-44*, pp. 75-81, Jet Propulsion Laboratory, Pasadena, Calif., Apr. 15, 1978.

Table 1. Geometry and basic assumptions

Satellite inclination from equator plane = 45°
Satellite inclination from plane of sky = 63°
Station latitude = 35°
Spacecraft declination = 0°
S/C-quasar angular separation = 20°
Solar-earth-S/C angle = 10°
S/C elevation at station = 25°
Quasar elevation at station = 40°
Solar-zenith angles of ionospheric reference points = 50° (S/C) 52° (quasar)
Quasar angular position error = 5 nrad
S/C angular position error = 150 nrad (for angle rate determination)
S/C-quasar angular separation error = 40 nrad (for angle rate determination)
Satellite position error in HCL = (1 m, 1 m, 3 m)
Satellite velocity error in HCL = (0.1 mm/s, 0.1 mm/s, 0.3 mm/s)
Station location error (including polar motion and UT1) = 50 cm in each direction
Zenith troposphere errors: 6 cm systematic 2 cm inhomogeneity
Zenith ionosphere errors: 1.5 cm peak 3 cm bias 3 cm spatial fluctuation 1 cm temporal fluctuation (600 sec)
Clock offset = 5 nsec
Frequency offset = 10 mHz at X-band
Clock instability = 10^{-13} over 600 sec at satellite 10^{-14} over 600 sec at station
Phase instability = 2°
Quasar correlated flux density = 0.2 Jansky
S/C power at satellite receiver = -170 dBm
RF frequency = 8.4 GHz (X-band)
Spanned bandwidth = 100 MHz
Channel bandwidth = 2 MHz
Antenna diameters = 28 m at satellite 34 m at station
Antenna efficiencies = 0.40 at satellite 0.55 at station
System temperature = 100 K at satellite 25 K at station
Observation time per source per baseline = 600 sec
Separation time between S/C and quasar observations = 720 sec

Table 2. Definition of symbols

a = satellite orbit radius = 4.22×10^9 cm	$\Delta f/f$ = clock instability in terms of Allan variance (RSS of both sites)
B = length of baseline projection on plane of sky, km	ϵ_{STN} = station location error, cm
c = speed of light = 3×10^{10} cm/sec	$\epsilon_H \epsilon_C \epsilon_L$ = satellite position errors in altitude, cross-track and in-track, cm
D = antenna diameter, m	$\epsilon_{\dot{H}} \epsilon_{\dot{C}} \epsilon_{\dot{L}}$ = satellite velocity errors, cm/sec
e = antenna efficiency	ϵ_ϕ = phase instability, rad
f_{ch} = channel bandwidth, Hz	ϵ_θ = S/C angular position error, rad
f_{off} = frequency offset between ground station and satellite, Hz	$\epsilon_{\theta, Q}$ = quasar angular position error, rad
f_{RF} = nominal RF frequency, Hz	$\epsilon_{\Delta\theta}$ = error in S/C-quasar angular separation, rad
f_{span} = spanned bandwidth, Hz	ϵ_τ = error in delay, cm
$f(X)$ = solar-zenith angle factor of ionosphere	$\epsilon_{\Delta\tau}$ = error in differenced delay, cm
$g(\gamma)$ = elevation angle factor of ionosphere	$\epsilon_{\dot{\tau}}$ = error in delay rate, cm/sec
k = Boltzmann constant = 1.38×10^{-23} Joule/K	$\epsilon_{\Delta\dot{\tau}}$ = error in differenced delay rate, cm/sec
P_t = received S/C tone power, watt	$\epsilon_{\dot{\theta}}$ = error in angle rate, rad/sec
S_c = correlated flux density of quasar signal, Jansky	$\epsilon_{\Delta\dot{\theta}}$ = error in rate of angular separation, rad/sec
SEP = solar-Earth-S/C angle, radian	ρ_{peak}^i = zenith ionospheric peak error, cm
SNR = ratio of correlated fringe amplitude to RMS noise	ρ_{bias}^i = zenith bias ionospheric error, cm
T_{obs} = observation time per source per baseline, sec	ρ_{spa}^i = zenith ionospheric spatial fluctuation, cm
T_{off} = clock offset between ground station and satellite, sec	ρ_{temp}^i = zenith ionospheric temporal fluctuation, cm
$T_{S/C-Q}$ = separation time between the middles of S/C and quasar observations, sec	ρ_z^t = zenith tropospheric error, cm
T_S = system noise temperature, K	ρ_{inh}^t = zenith tropospheric horizontal inhomogeneity, cm
V_{SW} = solar wind velocity = 400 km/sec	Ω = satellite inclination angle from plane of sky
X = solar-zenith angle of ionospheric reference point	ω_e = Earth's spinning rate, also satellite rotation rate
α, δ = S/C right ascension and declination	= 73×10^{-6} rad/sec
γ = elevation angle	
$\Delta\alpha, \Delta\delta$ = angular separation in α and δ between S/C and quasar, radian	

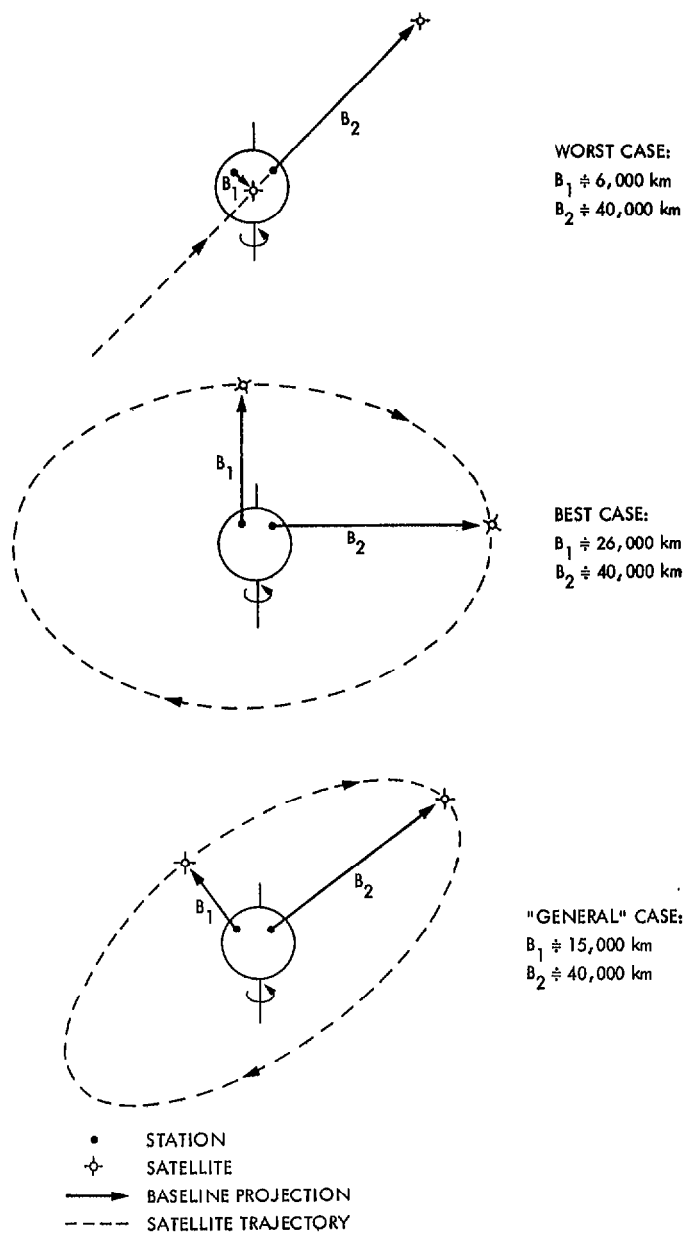


Fig. 1. Baseline projections on the plane of the sky

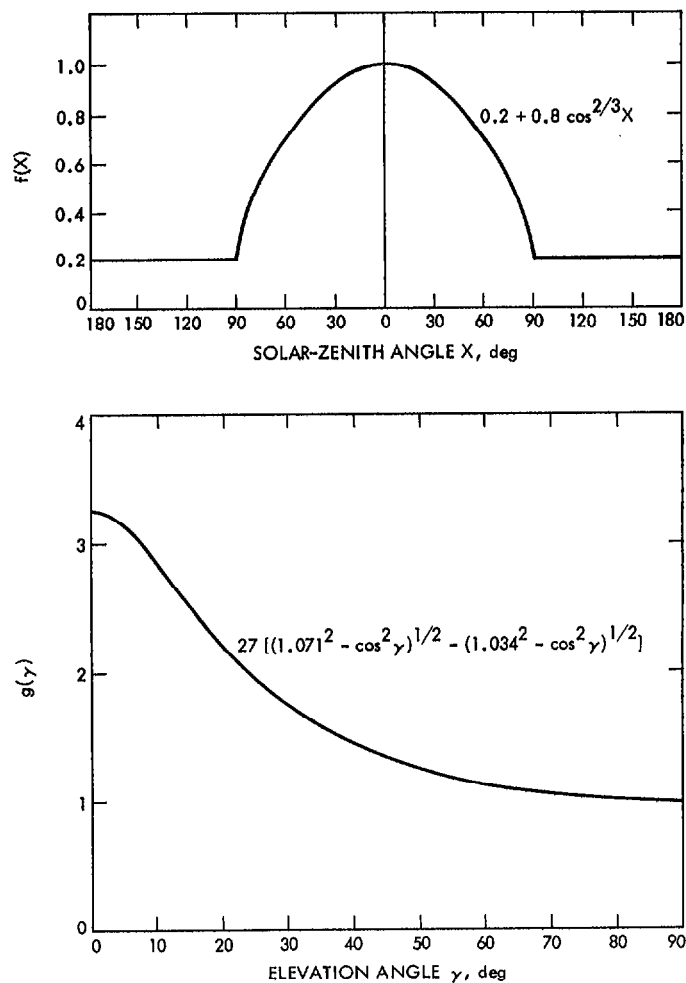


Fig. 2. Solar-zenith angle factor and elevation angle factor for ionospheric delay errors

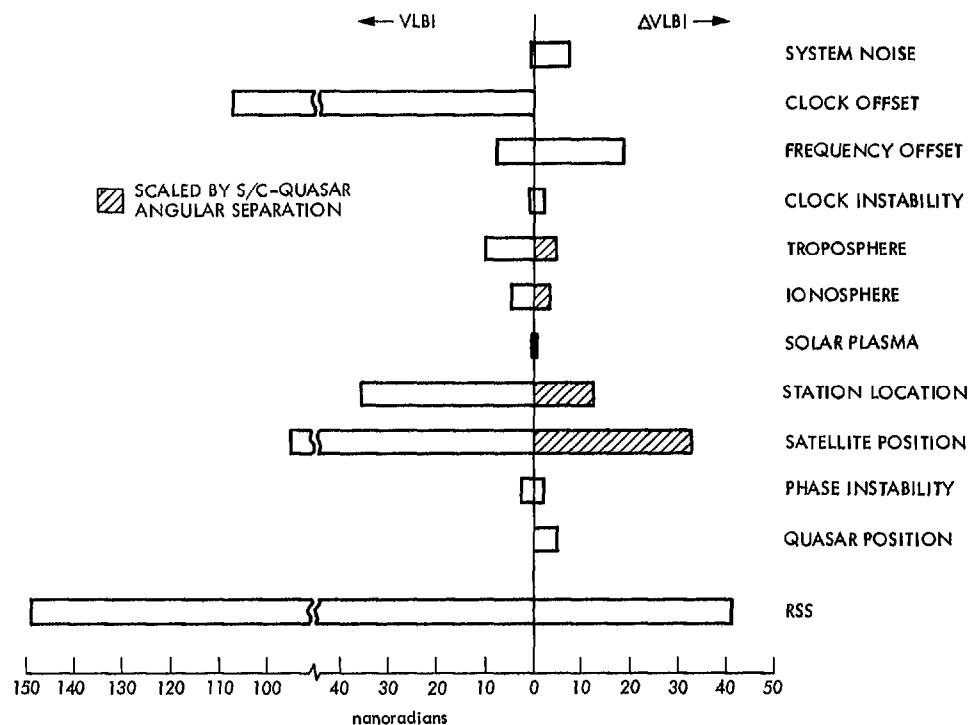


Fig. 3. Angle measurement errors from S/C-only VLBI and S/C-quasar Δ VLBI

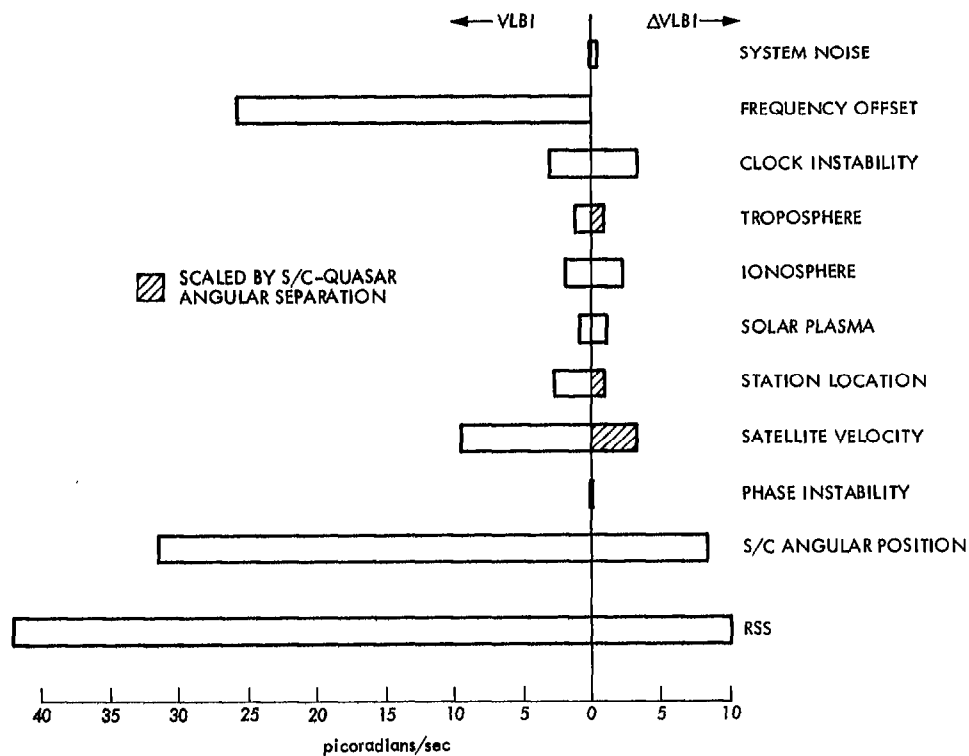


Fig. 4. Angle rate measurement errors from S/C-only VLBI and S/C-quasar Δ VLBI